Available online at www.sciencedirect.com

ScienceDirect

Procedia Structural Integrity 5 (2017) 85–92

Structural Integrity Procedia

www.elsevier.com/locate/procedia

2nd International Conference on Structural Integrity, ICSI 2017, 4-7 September 2017, Funchal, Madeira, Portugal

Plasticity induced closure under variable amplitude loading in AlMgSi aluminum alloys

L.F.P. Borrego[a,b]*, J.D. Costa[a], JA.M. Ferreira[a]

[a] *CEMMPRE, University of Coimbra, Department of Mechanical Engineering, Rua Luís Reis Santos, 3030-788, Coimbra, Portugal*
[b] *Instituto Politécnico de Coimbra, ISEC, Department of Mechanical Engineering,Rua Pedro Nunes, 3030-199 Coimbra, Portugal*

Abstract

Fatigue crack propagation tests under peak overloads, as well as High-Low and Low-High block loading sequences have been performed in aluminum alloy specimens. The observed transient crack closure level is discussed in terms of loading sequence, load change magnitude and ΔK baseline levels. The crack closure level is compared with the crack growth transients. A good agreement between experimental and predicted crack growth rates is obtained when the partial crack closure effect is properly taken into account. Therefore, plasticity-induced crack closure plays an important role on the load interaction effects observed in aluminum alloys.

Peer-review under responsibility of the Scientific Committee of ICSI 2017

Keywords: Damage Tolerance Overloads, block loading, partial crack closure, plasticity-induced crack closure

1. Introduction

Service conditions generally involve random or variable amplitude, rather than constant amplitude loads. Significant accelerations and/or retardations in crack growth rate can occur as a result of these load variations. Thus, an accurate prediction of fatigue life requires an adequate evaluation of these load interaction effects. To attain this objective several type of simple variable amplitude load sequences must be analyzed. Several mechanisms have been proposed to explain the crack growth transients following variable amplitude loading sequences, which includes

* Corresponding author. Tel.: +351 962560101; fax: +351 239790331.
E-mail address: borrego@isec.pt

2452-3216
Peer-review under responsibility of the Scientific Committee of ICSI 2017
10.1016/j.prostr.2017.07.072

models based on residual stress; crack closure; crack tip blunting; strain hardening, crack branching and reversed yielding. However, the precise micromechanisms responsible for these phenomena are not fully understood.

Crack closure has played a central role in the study of fatigue crack propagation, Elber (1970). Generally, under constant amplitude loading, closure measurements produce good correlation between low stress ratio and high stress ratio crack growth rate data, e.g. Blom and Holm (1985), Elber (1971), Borrego et al (2001), through the effective range of K corresponding to a fully open crack, ΔK_{eff}, introduced by Elber (1971).

In spite of some controversy, the effect of residual plastic deformation, which leads to compressive stresses before the crack-tip and raises the crack opening load on subsequent crack growth (crack closure), has been identified as the most important aspect in explaining also the characteristic features of crack growth retardation. However, under constant amplitude loading at the near-threshold regime the measured opening loads are sometimes excessively high because the role of the lower portion of the loading cycle below Kop to the fatigue crack growth behavior is not taken into account, e.g. Hertzberg et al (1988) and Chen et al (1996), resulting in a significant underestimation of the effective crack driving force. Additionally, under single peak overloads some discrepancies appear when the experimental post-overload transients are compared with crack growth rates inferred from remote closure measurements and the da/dN versus ΔK_{eff} relation for the material, Dexter et al (1989), Fleck (1988), Shercliff and Fleck (1990), Shin and Hsu (1993). Among other observations, these behaviors have contributed for some of the controversy around the phenomenon of crack closure.

The present work intends to analyses the crack closure levels on aluminum alloy specimens subjected to several variable amplitude loading sequences and evaluate if the observed transient crack growth behavior can be correlated with the crack closure phenomenon.

2. Material and experimental details

The material used in this research was an AlMgSi1 (6082) aluminum alloy with T6 heat treatment. The T6 heat treatment corresponds to a conversion of heat-treatable material to the age-hardened condition by solution treatment, quenching and artificial age-hardening. The alloy chemical composition and mechanical properties are shown in Table 1 and Table 2, respectively.

Table 1. Chemical composition of 6082-T6 aluminum alloy in wt.%.

Si	Mg	Mn	Fe	Cr	Cu	Zn	Ti	Al
1.05	0.80	0.68	0.26	0.01	0.04	0.02	0.01	Balance

Table 2. Monotonic properties of 6082-T6 aluminum alloy.

Tensile strength, σ_{uts} [MPa]	300±2.5
Yield strength, σ_{ys} [MPa]	245±2.7
Elongation, ε_r [%]	9

Fatigue tests were conducted, in agreement with ASTM E647 standard using Middle-Tension, M(T), specimens with 200 mm length, 50 mm width and 3 mm thickness. The specimens were obtained in the longitudinal transverse (LT) direction from a laminated plate. Fig. 1 illustrates the notch of the samples used in the tests. The notch preparation was made by electrical-discharge machining. After that, the specimen surfaces were mechanically polished.

All experiments were performed in a servo-hydraulic test machine interfaced to a computer for machine control and data acquisition. All tests were conducted in air, at room temperature and with a load frequency of 15 Hz. The specimens were clamped by hydraulic grips. The influence of the different loading sequences was investigated in the Paris regime at R=0.05. In all cases the crack growth rates were determined by the secant method.

During the single overload and load block tests the crack length was measured using a travelling microscope (45X) with a resolution of 10 μm. Collection of data was initiated after achieving an initial crack length of approximately 12 mm. The tests conducted under constant ΔK and stress ratio, R, conditions, were performed by manually shedding the

load with crack growth. The load shedding intervals were chosen so that the maximum ΔK variation was smaller than 2%.

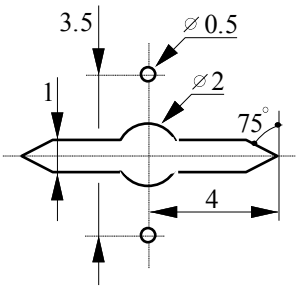

Fig. 1. Notch geometry of the M(T) specimen.

All the overloads performed both under load control as well as under constant ΔK and R conditions, were applied under load control during one cycle by programming the increase in load to the designated overload value. After overloading, the baseline loading was resumed and the transient crack growth behavior associated with the overload was carefully observed. Single tensile overload tests were performed at ΔK baseline levels, ΔK_{BL}, of 6 and 8 MPa√m. The overload ratio, OLR, was 1.5 and 2, which was defined as:

$$OLR = \frac{\Delta K_{OL}}{\Delta K_{BL}} = \frac{K_{OL} - K_{min}}{K_{max} - K_{min}} \tag{1}$$

where K_{max}, K_{min}, and K_{OL} are the maximum, minimum and peak overload intensity factors, respectively. The influence of the load blocks was investigated under High-Low (Hi-Lo) and Low-High (Lo-Hi) sequences, at ΔK baseline levels of 6, 9 and 12 MPa√m.

Load-displacement behavior was monitored at specific intervals throughout each of the tests using a pin microgauge elaborated from a high sensitive commercial axial extensometer. The gauge pins were placed in two drilled holes of 0.5 mm diameter located above and below the center of the notch. The distance between these holes was 3.5 mm. In order to collect as many load-displacement data as possible during a particular cycle, the frequency was reduced to 0.5 Hz. Noise on the strain gauge output was reduced by passing the signal through a 1 Hz low-pass mathematical filter.

Variations of the opening load, Pop, were derived from these records using the technique known as maximization of the correlation coefficient, Alison et al (1988). This technique involves taking the upper 10% of the load-displacement data and calculating the least squares correlation coefficient. The next data pair is then added and the correlation coefficient is again computed. This procedure is repeated for the whole data set. The point at which the correlation coefficient reaches a maximum can then be defined as P_{op}.

The fraction of the load cycle for which the crack remains fully open, parameter U, was calculated by the following equation:

$$U = \frac{P_{max} - P_{op}}{P_{max} - P_{min}} \tag{2}$$

where P_{max}, P_{min}, and P_{op} are the maximum, minimum and opening loads, respectively. The values of the effective K range parameter, ΔK_{eff}, were than calculated by the expression:

$$\Delta K_{eff} = K_{max} - K_{op} = U\,\Delta K \tag{3}$$

3. Results and discussion

3.1. Single tensile peak overloads under constant load conditions

Fig. 2 illustrates the typical transient crack growth behavior following single tensile overloads under constant-ΔP loading. In this figure the normalized crack growth ratio, $(da/dN)/(da/dN)_{CA}$, is plotted against the crack length from the overload event, $a\text{-}a_{OL}$, where $(da/dN)_{CA}$ is the constant amplitude crack growth rate at the same ΔK and a_{OL} the crack length at which the overload is applied. The ratio $(da/dN)/(da/dN)_{CA}$ is used instead of da/dN in order to simplify the comparison between the effects of overloads applied at different ΔK values. The depicted data were obtained for 50% and 100% intensity peak overloads (OLR values of 1.5 and 2, respectively) applied when ΔK=6 MPa√m or ΔK=8 MPa√m were achieved under constant amplitude loading.

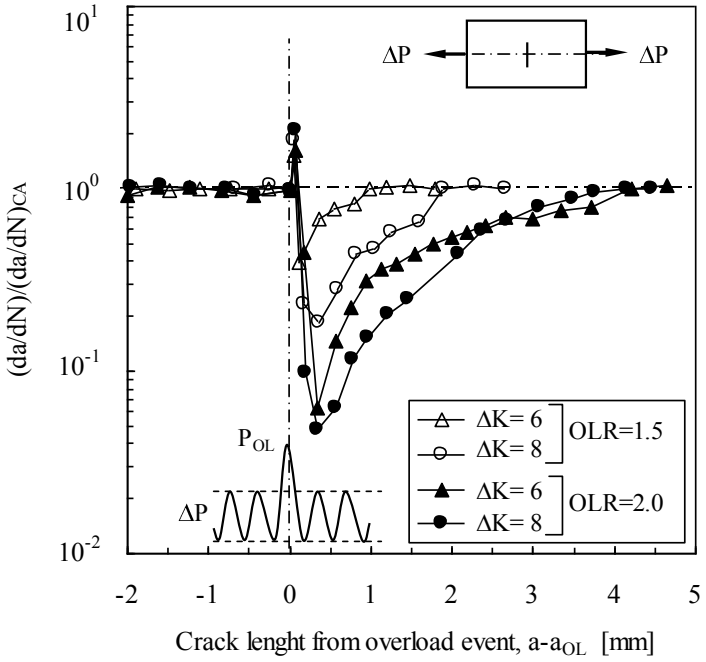

Fig. 2. Typical crack growth transient behavior after a single tensile overload.

There is a brief initial acceleration of crack growth rate immediately after the overload. The subsequent crack growth rate decreases until its minimum value is reached, followed by a gradual approach to $(da/dN)/(da/dN)_{CA}=1$, in other words, to the correspondent crack growth rate level obtained under constant amplitude loading. This trend is consistent with the behavior normally reported in the literature, Dexter et al (1989), Fleck (1988), Shercliff and Fleck (1990), Shin and Hsu (1993). The observed behavior is usually referred to as delayed retardation of crack growth. These figures show that the amount of crack growth retardation increases as the level of the overload ratio and also ΔK baseline levels increase. However, this last trend is also generally dependent of other parameters, Borrego et al (2003)

The correspondent crack closure data are presented in Fig. 3, plotted in terms of the load ratio parameter U, calculated by Eq. (2), against the crack growth increment from the point of overload application. This figure presents the typical crack closure response obtained following single tensile peak overloads under constant-ΔP loading. The stable crack closure level obtained under constant amplitude loading for ΔK values above 6 MPa√m [7] is also superimposed in the figure.

It is clear from this figure that the crack closure data show basically the same trend as the corresponding experimentally observed crack growth rate response presented in Fig. 2. Prior to the overload the U parameter is

relatively stable and approximately the same as for constant amplitude loading. Upon application of the overload, U rapidly increases followed by a decrease to a minimum value and then increases gradually towards the constant amplitude level**.**

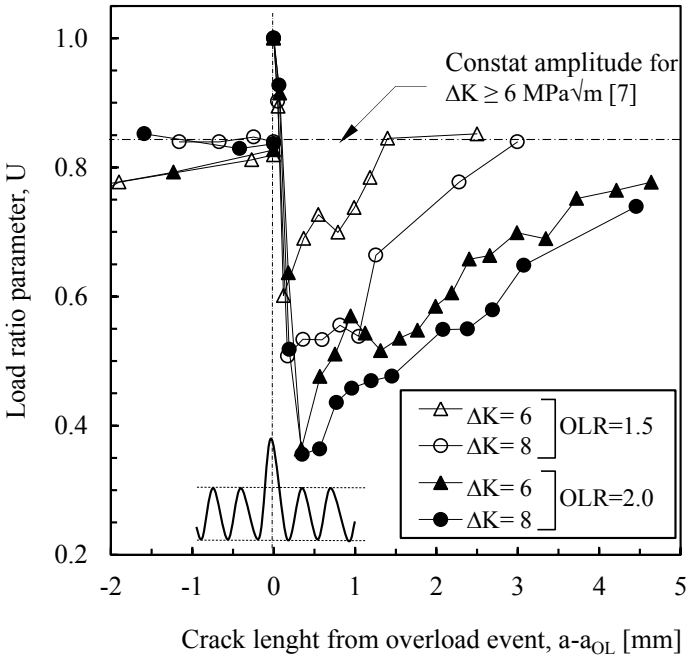

Fig. 3. Crack closure response after peak overloads applied under constant-ΔP loading.

It is important to notice that the decrease in U is not immediate after the overload application, which is in accordance with delayed retardation behavior observed on crack growth rate transients. Moreover**,** the results presented in Fig. 3 show clearly that in general the load parameter U decreases, in other words*,* the crack closure level increases, with increasing overload ratio and also with increasing ΔK at overload application. When U decreases the minimum effective driving force behind the crack is also decreased. The corresponding crack growth rates must therefore be lower. Thus, the observed effect of the severity of the overload, as well as the effect of the constant amplitude ΔK at which the overload is applied, on the crack retardation behavior is in accordance with the variation of the crack closure level. An increase in OLR or of ΔK increases the crack closure level, and therefore, the retardation effect should be more pronounced as indeed observed in Fig. 2.

However, the comparison between Fig. 2 and Fig. 3 indicates that for all the overloads, parameter U only reaches the corresponding constant amplitude level at a crack displacement after overloading, a-a_{OL}, higher than the overload affected crack growth increment, Δa_{OL}.

In order to clarify this behavior, fatigue crack growth tests under constant ΔK conditions were performed, resulting in controlled constant-crack-wake history, which is more sensitive to changes in fatigue crack growth rates associated with changing driving force mechanisms than constant-ΔP tests.

3.2. Single tensile peak overloads under constant-ΔK loading

Fig. 4 illustrates the typical crack closure response obtained following tensile peak overloads applied under constant-ΔK loading. The obtained data are plotted in terms of the normalized load ratio parameter U, calculated by Eq. (2), against the crack growth increment from the point of overload application, a-a_{OL}.

Prior to the overload the crack closure level at the baseline loading level is relatively stable. Upon application of the overload the load ratio parameter *U* rapidly increases, in other words, the crack closure level decreases, followed

by a decrease to a minimum value, U_{min}, *i.e.*, the crack closure level increases to a maximum, and then U increases, *i.e.*, the crack closure level decreases, gradually towards the corresponding value of the baseline level. Once again it is important to notice that the decrease in U is not immediate after the overload application, but on the contrary decreases slowly towards the minimum value. This is in accordance with delayed retardation behavior generally observed on crack growth rate transients, Shercliff and Fleck (1990) and Shin and Hsu (1993). Similar to the observed for overloads applied under constant load control, the pre-overload value is not attained at least until a crack increment after overloading much higher than the corresponding overload affected crack growth increment, Δa_{OL}, is reached Borrego et al (2003),. This fact was already attributed to the phenomenon of partial closure Fleck (1986), Tsukuda et al (1996), Borrego et al (2003), Borrego et al (2008), Borrego et al (2012). The results presented in Fig. 4 show that in general the normalized load parameter U decreases, *i.e.*, crack closure increases, with increasing overload ratio and ΔK baseline level.

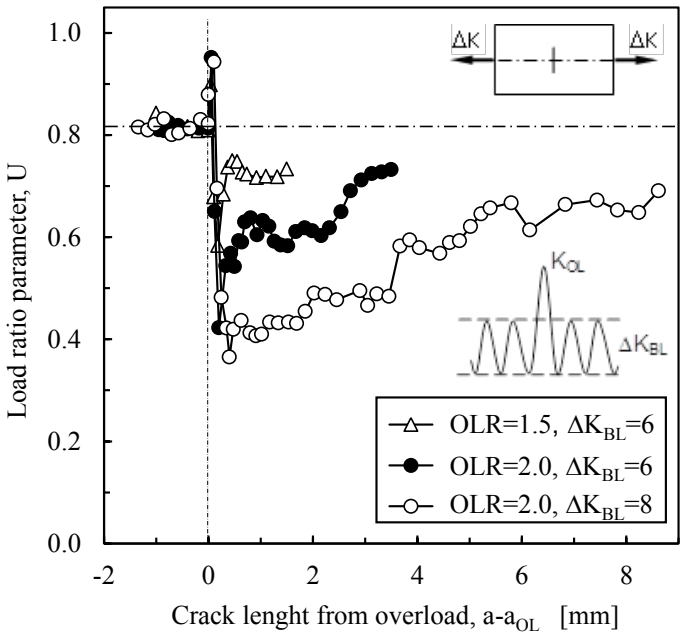

Fig. 4. Typical crack closure response following peak overloads applied under constant-ΔK loading.

3.3. Load step block sequences

Fig. 5 illustrate the typical crack closure response obtained following Hi-Lo and Lo-Hi block sequences, respectively. The obtained data are plotted in terms of the normalized load ratio parameter U, against the crack length from load step event, a-a_O.

Prior to the load step the U parameter at the baseline loading level is relatively stable (U≈0.83). Similarly to peak overloads, after load step-down U drops very quickly, *in other words*, the crack closure level increases, while after load step-up this parameter rapidly increases, *i.e.*, the crack closure level decreases. For both load sequences, this initial phase is followed by a period where parameter *U* tends gradually towards the stable crack closure level corresponding to the subsequent loading level of the block sequences. Contrary to the behavior observed after overloading, under Hi-Lo block sequences the decrease in U towards the minimum value is immediate after load step-down. Furthermore, this figure shows that under load step-down sequences with equal decrease in load (3 MPa√m), the crack closure level increases with the initial *ΔK* level, ΔK_1, Under Lo-Hi blocks acceleration increases with the final ΔK.

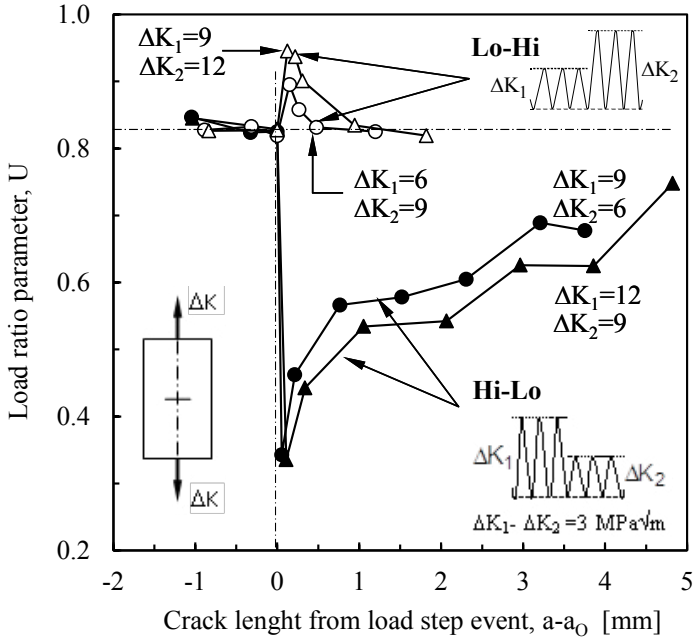

Fig. 5. Typical crack closure response under block loading.

4. Conclusions

From the study on the crack closure behavior in an aluminum alloy under several variable amplitude loading sequences, the following concluding remarks can be drawn:

1. Generally, the crack closure level variation is in agreement with the typical experimentally observed crack growth rate response.
2. Under peak overloads and Hi-Lo block sequences the crack opening load level indicated by a far field gauge (entire crack open) is not necessarily the actual crack opening load.
3. The plasticity-induced closure seems to be the main mechanism causing retardation.

Acknowledgements

The authors gratefully acknowledge the Portuguese Foundation for Science and Technology for funding the work reported, Project PTDC/EMS-PRO/3148/2012 co-financed by FEDER, through the Operational Factors for Competitiveness Programme of the QREN with reference COMPETE: FCOMP-01-0124-FEDER-029112.

References

Elber W. 1970. Fatigue crack closure under cyclic tension. Engng Fract Mech: 2: 37-45.

Blom AF, Holm DK. 1985. An experimental and numerical study of fatigue crack closure. Engng Fract Mech: 22: 997-1011.

Elber W. 1971. The significance of fatigue crack closure. In: Damage Tolerance in Aircraft Structures, ASTM STP 486. Philadelphia: American Society for Testing and Materials, pp. 230-242.

Borrego LP, Ferreira JM, Costa JM. 2001. Fatigue crack growth and crack closure in an AlMgSi alloy. Fatigue Fract Engng Mater Struct; 24:255-266.

Hertzberg RW, Newton CH, Jaccard R. 1988. Crack closure: correlation and confusion. In: Newman Jr JC and Elber W, editors. Mechanics of Fatigue Crack Closure, ASTM STP 982. Philadelphia PA: ASTM 1988. p. 139-148.

Chen DL, Weiss B, Stickler, R. 1996. Contribution of the cyclic loading portion below the opening load to fatigue crack growth. Mater Sci Engng; A208:181-187.

Dexter RJ, Hudak SJ, Davidson DL. 1989. Modelling and measurement of crack closure and crack growth following overloads and underloads. Engng Fract Mech;33:855-870.

Fleck NA. 1988. Influence of stress state on crack growth retardation. In: J. T. Fong and R. J. Fields, editors. Basic questions in fatigue: Volume 1, ASTM STP 924. Philadelphia PA: ASTM. p. 157-183.

Shercliff HR., Fleck NA. 1990. Effect of specimen geometry on fatigue crack growth in plane strain – II Overload response. Fatigue Fract Engng Mater Struct; 13: 297-310.

Shin CS, Hsu SH. 1993. 1988. On the mechanisms and behaviour of overload retardation in AISI 304 stainless steel. Int J Fatigue;15: 181-192.

Allison JE, Ku RC, Pompetzki MA. A comparison of measurement methods and numerical procedures for the experimental characterization of fatigue crack closure. In: Mechanics of Fatigue Crack Closure, ASTM STP 982. Newman Jr JC, Elber W (eds). Philadelphia PA, ASTM; p. 171-185.

Borrego LP, Ferreira JM, Costa JM. 2003. Evaluation of overload effects on fatigue crack growth and closure. Engng Fract Mech; 70: 1379-1397.

Fleck NA. 1986. Finite element analysis of plasticity-induced crack closure under plane strain conditions. Engng Fracture Mech; 25 (4): 441-449.

Tsukuda H, Ogiyama H, Shiraishi T. 1996. Transient fatigue crack growth behaviour following single overloads at high stress ratios. Fatigue Fract Engng Mater Struct; 19(7): 879-891.

Borrego LP, Ferreira JM, Costa JM. 2008. Partial crack closure under block loading. Int. J. Fatigue; 30: 1789-1796.

Borrego LP, Antunes FV, Costa JD, Ferreira JM. 2012. Numerical Simulations of Plasticity Induced Closure Under Overload and High-Low Blocks. Engng Fract Mech; 95: 57-71.